Designing broadband fiber optic parametric amplifier based on near-zero single ZDW PCF with ultra-flat nature

Partha Sona Maji and Ritwick Das*

School of Physical Sciences, National Institute of Science Education and Research, HBNI Bhubaneswar, Jatni 752050, India

**Corresponding author: ritwick.das@niser.ac.in*

Received December 29, 2016; accepted April 14, 2017; posted online May 10, 2017

We propose a broadband fiber optic parametric amplifier (FOPA) based on a near-zero ultra-flat dispersion profile with a single zero-dispersion wavelength (ZDW) by using a selective liquid infiltration technique. The amplifier gain and bandwidth is investigated for a variety of fiber lengths, pump power, and operating wavelengths. It is observed that sufficient peak gains and broader bandwidths can be achieved with a small negative anomalous dispersion ($\beta_2 \leq 0$) and a positive value of the 4th-order dispersion parameter ($+\beta_4$) around the pump. We can optimize an FOPA with a bandwidth of more than 220 nm around the communications wavelength.

OCIS codes: 060.4005, 060.5295, 190.4970, 230.2035.
doi: 10.3788/COL201715.070606.

Since the first realization of photonic crystal fibers (PCFs) around 1996[1], various novel PCF architectures have been investigated for different applications that are not possible with conventional step-index or graded-index fiber[2,3]. The unique properties of controllability of dispersion and superior nonlinearity with wideband single mode behavior[2–4] have made PCF a formidable choice for specific applications that are difficult to be realized with conventional waveguides[4–6]. For example, the conversion efficiency of four-wave mixing (FWM), which is the underlying mechanism for achieving a broadband fiber optic parametric amplifier (FOPA), can be significantly enhanced with dispersion-engineered PCFs through appropriate tailoring the phase-matching condition[7]. Dispersion profiles of the ultra-flat near-zero nature could further be exploited for high gain and broadband parametric amplification that depends upon efficient FWM applications. Recently, dispersion profiles with a flat nature with three zero-dispersion wavelengths (ZDWs) were investigated for their amplification properties[8]. However, for practical purposes, three pump conditions could not be applied simultaneously. At a particular instance, only one ZDW could be targeted and thereby the amplification performance could only be available corresponding to that ZDW. Also, the flatness of the dispersion profile was compromised to accommodate three ZDWs. At the same time, the wider ZDWs (2nd ZDW and 3rd ZDW) cease to exist for slightly higher temperature environments[9]. Since present dense wavelength division multiplexing (DWDM) systems require an increase of information capacity and thereby need amplifiers with uniform gain along with a wider bandwidth to compensate for the loss of fiber and equalize the power of the various channels, a wider bandwidth with a uniform gain is always in demand.

Even though dispersion can be tuned for specific applications, controlling dispersion for a wide wavelength range with all uniform air-hole diameters has been a difficult task. A few of the major architectures used in designing ultra-flat dispersion profiles have been like triangular doped core[10], different core geometries[11,12], or different types of air holes as well as the submicron size of air holes in the cladding of the fiber[13–16]. However, the technology in precisely realizing the ultra-flat nature is not easily feasible with the present-day fabrication technology. The selective liquid technology technique[17–23] has emerged as an alternative to the above issue since the mismatch in the optimized dispersion profile can always be compensated with different types of available liquids while at the same time fine tuning the profile for a change of the system temperature.

This Letter utilizes the selective liquid infiltration technique for designing a near-zero ultra-flat dispersion profile with a single ZDW with all uniform air-hole diameters in the cladding around the communications wavelength. This has been further applied toward a broadband FOPA. With the liquid infiltration technique, we could optimize an ultra-flat dispersion profile with $D = 0 + 1$ ps/(nm · km) for a bandwidth of 316 nm with all equal air-hole diameters in the cladding. The phase-matching condition of an optimized PCF has been employed to carry out parametric amplification after establishing the gain and bandwidth dependence upon fiber length, pump power, and operating wavelength. Our numerical investigation reports that with the proper choice of pump we could achieve a wide bandwidth FOPA source more than 220 nm around the communications wavelength.

The basic mechanism leading to the amplification in the degenerate FWM process is the conversion of two pump photons of frequency ω_p into a signal photon ($\omega_s < \omega_p$) and an idler photon ($\omega_i > \omega_p$) satisfying the energy conservation relation ($2\omega_p = \omega_s + \omega_i$), where subscripts "s",

 © 2017 Chinese Optics Letters

"i", and "p" stand for signal, idler, and pump, respectively. Efficient FWM, and thereby a high gain and wide bandwidth of FOPA, demands that a certain phase-matching condition is satisfied between the pump, the signal, and the idler.

The optical parametric gain G_s[7,24] is calculated using

$$G_s = 1 + \left(\frac{\gamma P}{g}\right)^2 \sinh^2(gL), \tag{1}$$

where γ is the effective nonlinear coefficient given by $\gamma = 2\pi n_2/(\lambda A_{\text{eff}})$ with n_2 is the nonlinear refractive indices (RIs); P is the input pump power; A_{eff} is the effective area and g is the parametric gain coefficient given by

$$g = \sqrt{(\gamma p)^2 - (\Delta k/2)^2},\ \Delta k = 2\gamma P + \Delta k_{\text{L}}, \tag{2}$$

where Δk_{L} is the linear phase-mismatch term $\Delta k_{\text{L}} = \Delta\beta + \Delta k_{\text{W}}$. The waveguide phasemismatch term Δk_{W} can be neglected for single-mode fibers[7] and, considering up to the 4th order, $\Delta\beta$ can be written as[7]

$$\Delta\beta = \beta_2(\Delta\omega)^2 + \frac{1}{12}\beta_4(\Delta\omega)^4 \tag{3}$$

where $\Delta\omega$ is the frequency shift ($\Delta\omega = \omega_{\text{p}} - \omega_{\text{s}} = \omega_{\text{i}} - \omega_{\text{p}}$) and β_2 and β_4 are the 2nd and 4th orders of the dispersion parameter given by $\beta_2 = -\frac{\lambda^2}{2\pi c}D$ and $\beta_4 = \frac{D^2}{Dw^2}\beta_2$; D is the chromatic dispersion parameter given by $D = -\lambda/c\mathrm{d}^2\mathrm{Re}[n_{\text{eff}}]/\mathrm{d}\lambda^2$, where $\mathrm{Re}[n_{\text{eff}}]$ is the real part of the effective RIs obtained from simulation.

For the net OPA gain, the linear phase-mismatch term $\Delta\beta$ must be negative with sufficient magnitude to balance the nonlinear contributions, i.e., $\Delta\beta$ should satisfy the condition of $-4\gamma P \le \Delta\beta \le 0$. For perfect phase matching in Eq. (2), the value of Δk becomes zero, which in turn corresponds to the maximum signal gain. In this situation, $\Delta\beta = -2\gamma P$ with $g_{\max} = \gamma P$.

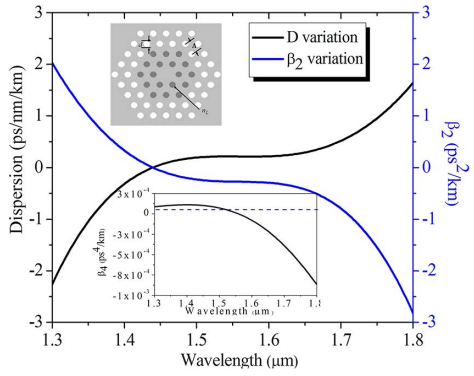

Fig. 1. (Color online) Optimized dispersion profile with $D = 0 + 1\,\text{ps}/(\text{nm}\cdot\text{km})$ over a wavelength range of 316 nm and corresponding β_2 variation. Top inset: the cross section of the optimized design. Bottom inset: the corresponding 4th-order GVD parameter (β_4), which remains positive up until the wavelength value of 1558 nm.

The investigated PCF schematic diagram is presented in the top inset of Fig. 1, with a silica background with two inner air-hole rings infiltrated with liquid of the chosen RI. For the ease of fabrication, the air-hole diameter is kept constant. The modal fields associated with dispersion and nonlinear properties are investigated using a multipole method-based solver[25]. Designing near-zero and ultra-flat PCFs for communications wavelengths is a task with optimization of multiparameters that include air-hole diameter (d), hole-to-hole distance (Λ), and liquid RI (n_{L}). The detailed investigation of the dependence of individual parameters on total dispersion and its slope is described in the supplementary information. We optimized an ultra-flat D profile with almost a flat slope and near-zero value with $D = 0 + 1\,\text{ps}/(\text{nm}\cdot\text{km})$ for a 316 nm (1440 to 1756 nm) wavelength range, as demonstrated in Fig. 1, with a propagation loss of $\sim 10^{-3}$ dB/m with $\Lambda = 3.05\,\mu\text{m}$ and $d = 1.52\,\mu\text{m}$ for a liquid of $n_{\text{L}} = 1.35$[26,27]. The value of the ZDW has been found to be 1440 nm for the above case. The corresponding variation of the higher-order group velocity dispersion (GVD) parameter of β_2 is presented in Fig. 1, while the variation of β_4 is presented in the bottom inset of Fig. 1. It is interesting to note that the value of β_4 remains positive until a wavelength of 1558 nm.

Proper FOPA performance depends upon the phase-matching condition (pump condition) as well as the dispersion profile of the working fiber. FOPA gain and bandwidth dependence is discussed below for a change of fiber length, pump power, and pump wavelength (λ_{p}).

The simulation for FOPA gain and bandwidth has been carried out using Eq. (1). To investigate the FOPA gain, the required parameters of nonlinear coefficient (γ) and parametric gain coefficient (g) are calculated as an initial step. The parameter "g" and the phase-mismatch factor term are evaluated as per Eq. (2) and the value of the higher-order dispersion parameter, which is required to calculate the phase-mismatch term $\Delta\beta$, is estimated according to Eq. (3). The values of β_2 and β_4 are estimated from the chromatic dispersion parameter (D).

The FOPA gain and bandwidth for a variation of fiber length around the ZDW are shown in Fig. 2 for a pump power of 10 W and input λ_p at 1450 nm for an anomalous

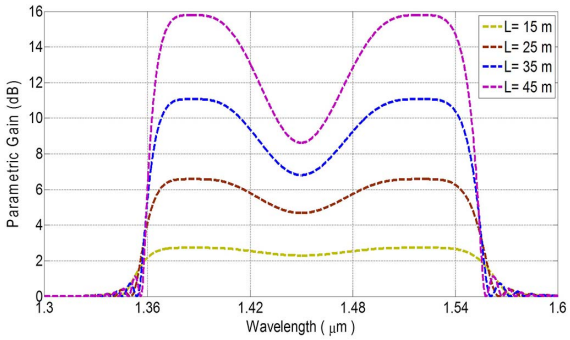

Fig. 2. (Color online) FOPA gain and bandwidth variation as a function of the fiber length for a fixed pump power of 10 W.

pumping. The FOPA gain increases with the fiber length, however, the bandwidth decreases due to an increase of phase mismatch for longer fibers. Additionally, matching of phase for an increased value of fiber length is broken owing to longitudinal chromatic dispersion fluctuation along the fiber length[28]. Consequently, a fiber length of 30–40 m will serve the purpose of a wider bandwidth of the FOPA. Since the studied fiber is having a propagation loss $\sim 10^{-3}$ dB/m, the aforementioned length contributes only a negligible loss for the signal propagation.

The FOPA gain for pump power variation is presented in Fig. 3 for 35 m of fiber length at $\lambda_p = 1450$ nm. It can be clearly observed that the gain as well as the bandwidth increases as a function of the pump power. However, the pump power necessarily needs to be optimized for suppressing nonlinear effects such as stimulated Raman scattering. In order to study the consequence of the above nonlinear effects, the Raman threshold (R_{Th}) has been computed in our FOPA configuration. Considering the Raman gain coefficient for silica is $\sim 10^{-13}$ m/W[7], the calculations show R_{Th} to be ~150 W (with a propagation length of 35 m) and accordingly a pump power of ~12 W will not be sufficient to induce any Raman effect. On a different note, the input intensity corresponding to the above pump power of optimized fiber is ~40 MW/cm^2. The value is much less than the R_{Th} of 0.6 GW/cm^2[7], ensuring no impact of Raman scattering.

The FOPA gain spectrum and the associated phase-mismatch term $\Delta\beta$ for a variation of λ_p with a pump power of 10 W and a fiber length of 40 m is shown in Figs. 4(a) and 4(b), respectively. Improved phase matching and consequent superior FOPA gain with wider bandwidth is achieved around smaller anomalous pumping (i.e., $\beta_2 \le 0$) having a positive β_4[28]. The bottom inset of Fig. 1 presents the optimized PCF having a $+\beta_4$ around the ZDW (up to 1558 nm). Since the optimized PCF is having a flat dispersion close to zero value, the pumping condition can be tuned further from the ZDW toward the anomalous region (with marginal alteration in $-\beta_2$ values) for an improved phase matching and consequent wider bandwidth with an adequate FOPA gain. Such a tunable pump source can be achieved by outcoupling the signal in an optical parametric oscillator (OPO) with proper valued of grating period and operating temperature[29]. Consequently, the ultra-flat nature of the optimized dispersion profile imparts an additional advantage where tuning of the pump wavelength adds additional degrees of freedom toward achieving high gain and a wider spectrum, which is explained in Fig. 4 as follows. We started our investigation with a normal dispersion pumping at 1438.5 nm (remember ZDW = 1440 nm) as presented with the red curve. It can be observed that the $\Delta\beta$ lies well above (actually, positive) the gain criteria of $-4\gamma P \le \Delta\beta \le 0$ [Fig. 4(b)] and as a consequence results in a very small gain and narrow bandwidth [red curve of Fig. 4(a)]. Moving toward a small anomalous pumping ($\lambda_p = 1342.5$ and 1346.5 nm), the $\Delta\beta$ variation is negative, however, it is yet to reach the maximum gain criteria of $\Delta\beta = -2\gamma P$ and consequently results in a smaller gain and narrower bandwidth, however, better than the normal pumping one ($\lambda_p = 1338.5$ nm). Moving further at $\lambda_p = 1350.5$ nm, the value of $\Delta\beta$ remains around $-2\gamma P$ for relatively wider wavelengths, resulting in almost a flat (variation is less than 1%) gain spectrum both in the idler and signal parts around 1370–1400 and 1505–1535 nm, respectively. It is interesting to observe that the wider spectrum with a maximum gain could be achieved for $\lambda_p = 1354.5$ nm as $\Delta\beta$ remains nearer to the favorable phase-mismatch

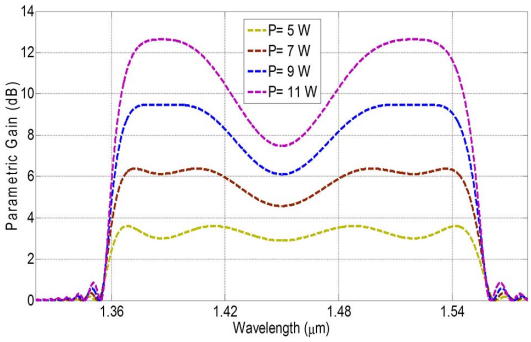

Fig. 3. (Color online) FOPA gain and bandwidth variation as a function of the pump power (P) for a 35 m fiber length at $\lambda_p = 1450$ nm.

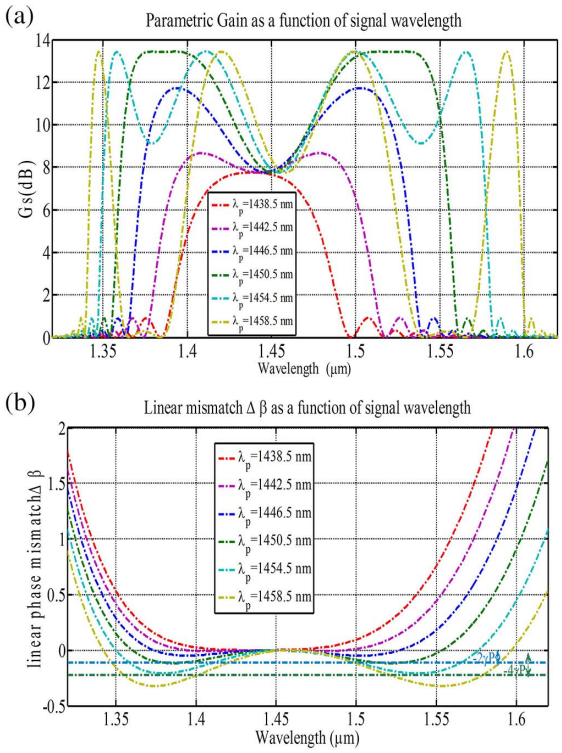

Fig. 4. (Color online) (a) FOPA gain and bandwidth variation as a function of pumping wavelength for a pump power of 10 W and a fiber length of 40 m around the ZDW. (b) The phase-mismatch ($\Delta\beta$) alteration corresponding to (a). The phase-mismatch curve clearly predicts the dip and peak of the FOPA gain spectrum.

condition of $-4\gamma P \le \Delta\beta \le 0$ and maximum gain took place at $\Delta\beta = -2\gamma P$ for a tuning of λ_p away from the ZDW. This is primarily a consequence of the near-zero ultra-flat nature of the dispersion profile with a negligible change in β_2. So broadband FOPA gain is achievable for $\Delta\beta$ lying closer to $-2\gamma P$ and the above finds practical realization by incorporating a proper choice of the pumping condition, which can be seen in Figs. 4(a) and 4(b) for the gain and phase-mismatch curve, respectively. Tuning λ_p further at 1458.5 nm, we can observe $\Delta\beta$ remain outside of the permissible limit of $-4\gamma P \le \Delta\beta \le 0$, and consequently this results in a narrower bandwidth. However, $\Delta\beta$ values $-2\gamma P$ around 1590 nm (upper wavelength of the spectrum) and 1340 nm (lower wavelength of the spectrum) for wider wavelengths for the same λ_p resulting in sharper peaks about these wavelengths, which can be clearly found from Figs. 4(a) and 4(b), respectively. So the bandwidth decreases, but we can realize new peaks on either side of the central spectrum far from the pump with a wide tuning from the ZDW. The above nature is interesting, since we can realize narrow peaks very far from λ_p with a proper choice of pump conditions. Thus, the phase-matching curve dictates completely the nature of the gain and bandwidth spectra of the FOPA performance. This principle of achieving wider FOPA gain with a $+\beta_4$ at a smaller anomalous pump condition can be applied for achieving high gain with a wider spectrum by means of the appropriate engineering of the waveguide geometry.

Based upon the FOPA gain and bandwidth variation for a change of fiber length, pump power, and pump wavelength, we optimized an FOPA gain spectrum, as presented in Fig. 5, with $P = 8.5$ W and 35 m long fiber at $\lambda_p = 1453.7$ nm. A wideband spectrum having a 3 dB bandwidth of 223 nm from 1352 to 1575 nm with a peak gain of 8.7 dB has been achieved. The equivalent phase-mismatch term has been depicted in the inset of Fig. 5. The phase-mismatch curve clearly predicts the dip and peak of the FOPA gain spectrum where proper gain took

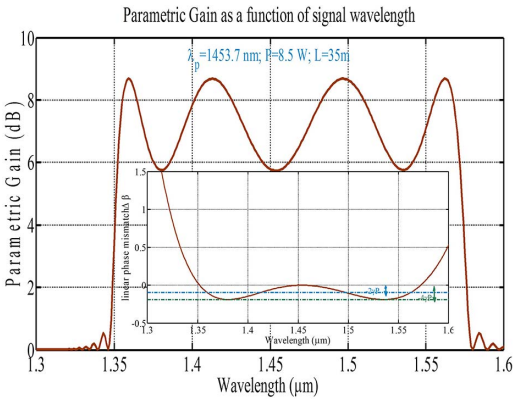

Fig. 5. Optimized parametric gain spectrum for a bandwidth of 223 nm. Inset: the corresponding $\Delta\beta$ variation. The net gain took place for $-4\gamma P \le \Delta\beta \le 0$ while the maximum gain corresponds to $\Delta\beta = -2\gamma P$.

place in the range $-4\gamma P \le \Delta\beta \le 0$ and peak gain took place for $\Delta\beta = -2\gamma P$.

In conclusion, this work presents realization of a broadband parametric amplifier based on a dispersion-engineered near-zero ultra-flat profile with selective liquid infiltration. We can optimize a dispersion profile with $D = 0 + 1$ ps/(nm · km) for a wavelength band of 316 nm with $\Lambda = 3.05$ μm and $d = 1.52$ μm and a practical liquid having an RI of 1.35 with a ZDW of 1440 nm. The relatively larger PCF parameters ensure that the optimized design can be realized in practice. The parametric gain and bandwidth is investigated in detail for a variation of PCF length, pump power, and pump wavelength. It is observed that increasing the length of the fiber increases the FOPA gain with reduced bandwidths, while an increment of the pump power leads to simultaneous increments of the gain and bandwidth. The pump wavelength dependence upon the FOPA gain and bandwidth reveals some unique outcomes. Our investigation reveals that an appropriate alteration of the pump wavelength improves the FOPA gain bandwidth by means of favorable higher-order dispersion parameters having $\beta_2 \le 0$ and $+\beta_4$ around ZDW. Based on the variation of the FOPA gain and bandwidth for a change of fiber length, pump power, and pump wavelength (λ_p), our numerical analysis established an optimized FOPA gain bandwidth of more than 220 nm around the ZDW.

P. S. M. thanks the Science & Engineering Research Board (SERB), New Delhi, India, for the NPDF fellowship (File No. PDF/2016/001827). Authors gratefully acknowledge the financial support received from National Institute of Science Education and Research (NISER), Department of Atomic Energy (DAE), Government of India.

References

1. J. C. Knight, T. A. Birks, P. St. J. Russell, and D. M. Atkin, Opt. Lett. **21**, 1547 (1996).
2. P. St. J. Russel, J. Lightwave Technol. **24**, 4729 (2006).
3. J. C. Knight, Nature **424**, 847 (2003).
4. B. Kuhlmey, G. Renversez, and D. Maystre, Appl. Opt. **42**, 634 (2003).
5. J. M. Dudley and J. R. Taylor, Nat. Photon. **3**, 85 (2009).
6. B. T. Kuhlmey, R. C. PcPhedran, C. M. de Sterke, P. A. Robinson, G. Remversez, and D. Maystre, Opt. Express **10**, 1285 (2002).
7. G. P. Agrawal, *Nonlinear Fiber Optics, Optics and Photonics Series*, 4th ed. (Academic Press, 2007).
8. P. S. Maji and P. R. Chaudhuri, Appl. Opt. **54**, 3263 (2015).
9. P. S. Maji and P. R. Chaudhuri, IEEE Photon. J. **7**, 1 (2015).
10. K. P. Hansen, Opt. Express **11**, 1503 (2003).
11. K. Saitoh, N. J. Florous, and M. Koshiba, Opt. Lett. **31**, 26 (2006).
12. N. J. Florous, K. Saitoh, and M. Koshiba, Opt. Express **14**, 901 (2006).
13. K. Saitoh and M. Koshiba, Opt. Express **12**, 2027 (2004).
14. K. Saitoh, M. Koshiba, T. Hasegawa, and E. Sasaoka, Opt. Express **11**, 843 (2003).
15. F. Poletti, V. Finazzi, T. M. Monro, N. G. R. Broderick, V. Tse, and D. J. Richardson, Opt. Express, **13**, 3728 (2005).
16. T.-L. Wu and C.-H. Chao, IEEE Photon. Technol. Lett. **17**, 878 (2005).
17. P. S. Maji and P. R. Chaudhuri, Opt. Comm., **325**, 134 (2014).

18. B. J. Eggleton, C. Kerbage, P. S. Westbrook, R. S. Windeler, and A. Hale, Opt. Express **9**, 698 (2001).
19. C. Yu and J. Liou, Opt. Express **17**, 8729 (2009).
20. S. Yiou, P. Delaye, A. Rouvie, J. Chinaud, R. Frey, G. Roosen, P. Viale, S. Février, P. Roy, J.-L. Auguste, and J.-M. Blondy, Opt. Express **13**, 4786 (2005).
21. C. Kerbage and B. J. Eggleton, Opt. Express **10**, 246 (2002).
22. M. Sasaki, T. Ando, S. Nogawa, and K. Hane, Jpn. J. Appl. Phys. **41**, 4350 (2002).
23. A. Witkowska, K. Lai, S. G. Leon-Saval, W. J. Wadsworth, and T. A. Birks, Opt. Lett. **31**, 2672 (2006).
24. M. Marhic, *Fiber Optical Parametric Amplifiers, Oscillators and Related Devices* (Cambridge University, 2008).
25. CUDOS MOF utilities available online: http://sydney.edu.au/science/physics/cudos/research/mofsoftware.shtml.
26. K. M. Gundu, M. Kolesik, J. V. Moloney, and K. S. Lee, Opt. Express **14**, 6870 (2006).
27. http://www.cargille.com/.
28. S. K. Chatterjee, S. N. Khan, and P. R. Chaudhuri, Opt. Commun. **332**, 244 (2014).
29. M. K. Shukla, P. S. Maji, and R. Das, Opt. Lett. **41**, 3033 (2016).